



University
of Glasgow

Konda, P. C. , Taylor, J. and Harvey, A. R. (2017) Fourier Ptychography with Scheimpflug Optics for Multi-Aperture Applications. Imaging and Applied Optics 2017, San Francisco, CA, USA, 26-29 Jun 2017.

There may be differences between this version and the published version. You are advised to consult the publisher's version if you wish to cite from it.

<http://eprints.gla.ac.uk/143997/>

Deposited on: 12 July 2017

Enlighten – Research publications by members of the University of Glasgow
<http://eprints.gla.ac.uk>

Fourier ptychography with Scheimpflug optics for multi-aperture applications

Pavan Chandra Konda, Jonathan M. Taylor, Andrew R. Harvey*

Imaging Concepts Group, School of Physics and Astronomy, University of Glasgow, Scotland, G12 8QQ, UK

**Andy.Harvey@glasgow.ac.uk*

Abstract: We present a new optical configuration using the Scheimpflug principle for Fourier ptychography microscopy. This configuration minimizes the aberrations present in the off-axis lenses of a multi-aperture Fourier ptychography setup. A 3D printed setup was used to demonstrate the experimental implementation.

OCIS codes: (100.5070) Phase retrieval; (170.0180) Microscopy; (110.1758) Computational imaging

1. Introduction

Fourier ptychography (FP) microscopy [1] was proposed recently to achieve space-bandwidth product in the gigapixel range. FP is a synthetic aperture technique which exploits Ewald sphere theory to shift the frequency spectrum permitted through the passband of the optical system. This is achieved by time-sequential simulation of a high-NA illumination using an LED array. Due to the time-sequential nature of the technique FP suffers from long data-acquisition times. Multi-aperture Fourier ptychography (MAFP) [2,3] was proposed by us to parallelize the data capture using an array of cameras, hence improving the acquisition times. When combined with multiplexed illumination [4], MAFP systems can capture several FP datasets per second depending on the hardware. On the other hand, MAFP suffers from aberrations in the off-axis camera systems [5] which degrades the quality of the reconstructed images in high-NA systems. As a solution to this problem we proposed to implement Scheimpflug optics for the off-axis camera systems in order to minimise these aberrations [3], thus improving the MAFP system performance in high-NA configurations. In this manuscript, we describe details about the Scheimpflug configuration for FP and present an experimental validation.

In the next section we describe the Scheimpflug principle and its application for FP. We then present details about the experimental setup built using 3D printed parts. We later present experimental results validating the Scheimpflug configuration for FP. In the future, this configuration will be applied to an MAFP setup for high-NA applications.

2. Scheimpflug Fourier ptychography principle

The Scheimpflug principle was developed to correct for perspective distortion when imaging tall structures from close range. The principle states that if the lens is tilted with respect to the object, then the detector must also be tilted with respect to both, the object and the lens such that the detector plane must pass through the intersection of the lens plane and the object plane. This can be seen in the Scheimpflug FP configuration shown in Fig. 1 (b) brown camera system. The position of the off-axis Scheimpflug lens and detector are given by the following equations:

$$L_s = \frac{1+m_o}{m_o} f \sin \theta_l, \quad (1) \quad L_h = \frac{1+m_o}{m_o} f \cos \theta_l, \quad (2)$$

$$D_s = \frac{(1+m_o)^2}{m_o} f \sin \theta_l, \quad (3) \quad D_h = \frac{(1+m_o)^2}{m_o} f \cos \theta_l, \quad (4)$$

$$\theta_d = \arctan \frac{(1+m_o) \cos \theta_l}{1-(1+m_o) \sin \theta_l}, \quad (5)$$

Where, L_s and D_s denote the distances from the central optical axis to the centre of the lens and the detector respectively; L_h and D_h denote the height of the lens and the detector from the object plane respectively; θ_l and θ_d

denote the angle of the lens and the detector with respect to the object plane; m_o is the magnification of the off-axis system and f is the focal length of the off-axis lens.

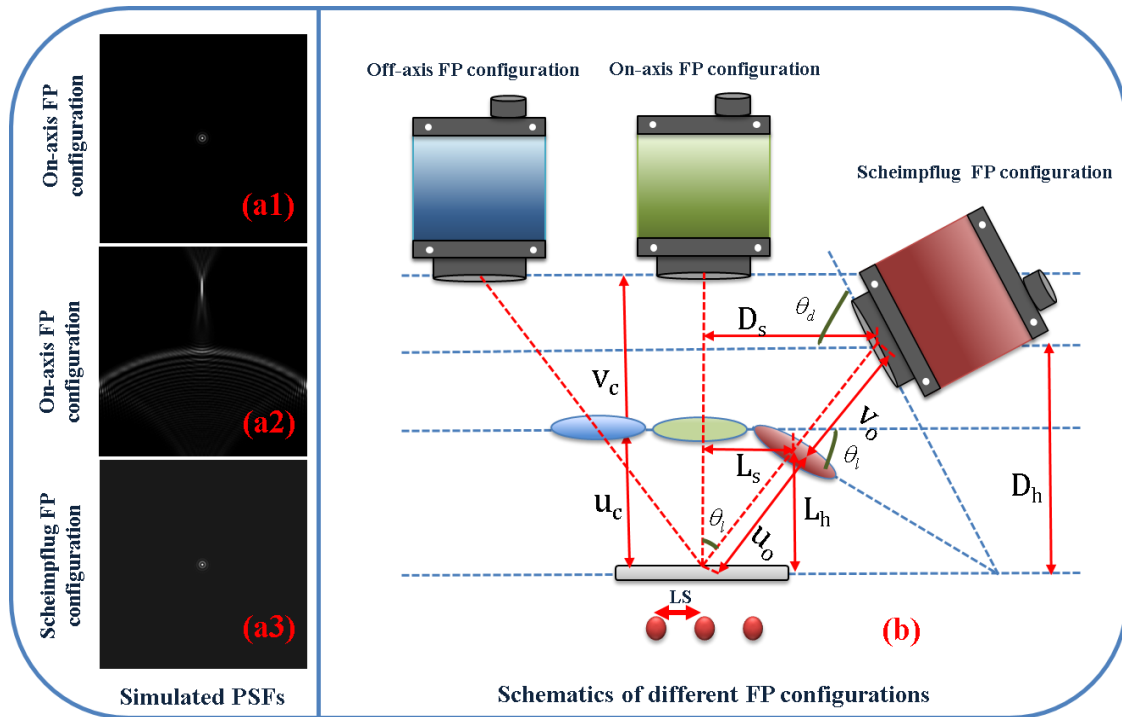


Figure 1 Scheimpflug FP setup geometry showing the positions of the imaging lenses and the detectors. On-axis and off-axis FP systems are shown for comparison. The psfs of these systems are shown in a1-a3.

Fig. 1 outlines the different types of FP configurations that can be implemented in an MAFFP setup. The camera system in green is a conventional FP system configuration used for the central camera of MAFFP systems. In this configuration the lens is parallel to the object plane and the detector plane. The object, the lens and the detector are centred on the optical axis of the system. This system does not have any aberrations; hence, the point spread function (psf) which is shown in Fig. 1 (a1) is ideal. The camera system in blue is an off-axis FP configuration used in the planar MAFFP setup demonstrated in [5]. In this configuration, the lens the object and the detector are parallel to each other which is similar to previous configurations; however, unlike the central camera system the object and detector are off-centred from the optical axis of the off-axis lens. This permits the capture of high spatial frequency information about the object and increases the bandwidth in an MAFFP system. This configuration, however, suffers from severe aberrations due to the off-axis nature of the system which is seen in the psf shown in Fig. 1 (a2). The camera system in brown is an off-axis FP system with Scheimpflug optical configuration. In this configuration, the lens is off-centred from the object but also tilted at the same time with respect to the object. This forms an image in a plane which is also tilted with respect to both object and lens where the angle of the detector is given by the Scheimpflug principle explained later. This configuration minimises the aberrations in the off-axis system which can be observed in the psf shown in Fig. 1 (a3). This psf is very similar to the on-axis FP system hence resulting in high quality images for MAFFP systems. The psfs in Fig. 1 were simulated using Zemax and the separation between the lenses was chosen as 15mm according to the experimental design.

3. Experimental setup and results

An experimental setup to implement Scheimpflug FP in an MAFFP system was built using 3D printed components as shown in Fig. 2. The lenses were placed at an angle in a 3D printed mount and a 3-axis kinematic stage was developed to mount the detector. The sample was placed on an XYZ translation stage and illuminated by an Adafruit LED array which has an LED separation of 5mm. The LED array was placed 125mm below the sample. Achromatic lenses with a focal length of 36mm and an aperture diameter of 8mm were utilised as imaging lenses. The separation between the lenses was set at 15mm such that a 7x7 LED array can cover the missing frequencies between the lenses

in the MAFP configuration. The numerical aperture of the low-NA system was 0.07. For Scheimpflug FP validation, one of the off-axis systems situated on the horizontal axis of the lens array was compared to the central camera system. A separate set of 7x7 LEDs from the array were chosen for each of these systems such that both of them record similar band of spatial frequency information.

A USAF resolution target was imaged to validate our system. In Fig 2. (a1) and (b1), the low-NA images from the central system and the Scheimpflug system are shown respectively. Their corresponding high-NA FP reconstruction images are shown in Fig. 2 (a2) and (b2) where a second order Gauss-Newton based reconstruction algorithm [6,7] was used to perform the reconstruction. It can be observed that the Scheimpflug FP reconstruction is comparable to that of the on-axis FP system. There are some minor artefacts in the higher group elements which are due to improper calibration of the system. We are currently working on improving the calibration of our system.

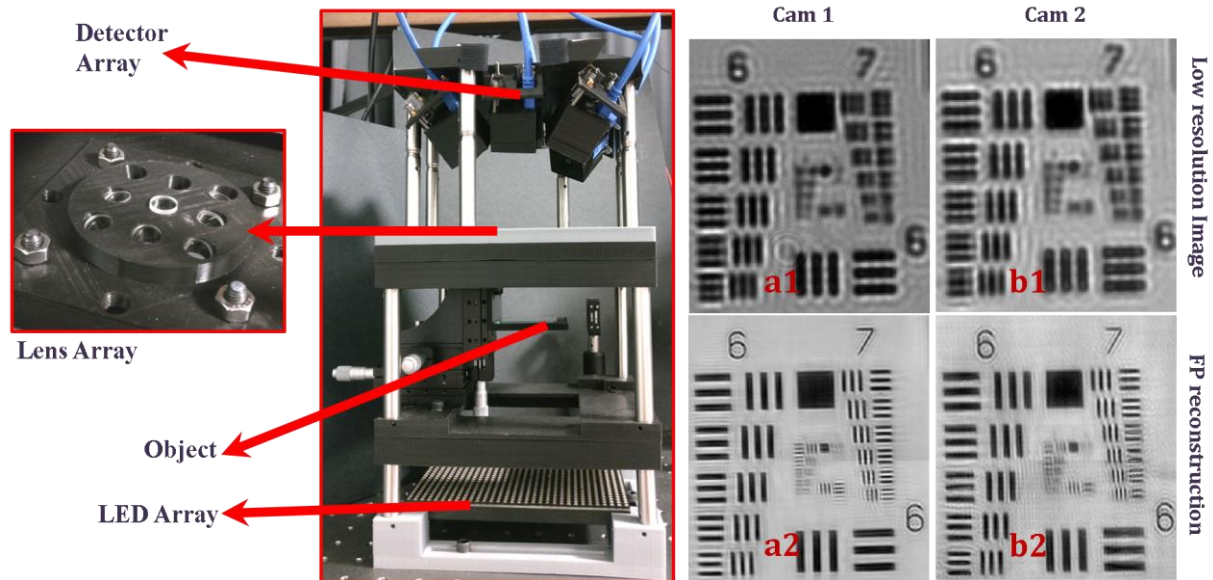


Figure 2 Experimental setup and results

4. Conclusion

In this work we have demonstrated a new optical configuration based on the Scheimpflug principle for off-axis FP systems. This configuration can be useful in building robust MAFP systems. We presented an experimental setup for Scheimpflug based MAFP using 3D printed components. We used one of the off-axis systems in this setup to validate the Scheimpflug principle for FP. Scheimpflug FP configuration can also be used to build high-NA tomography setup with multiple apertures.

5. References

1. R. Horstmeyer, G. Zheng, and C. Yang, "Wide-field, high-resolution Fourier ptychographic microscopy," *Nat. Photonics* **7**, 739–745 (2013).
2. P. Konda, J. Taylor, and A. R. Harvey, "Multi-aperture Fourier Ptychography imaging in the near field," in *Imaging and Applied Optics 2015, OSA Technical Digest (Online) (Optical Society of America, 2015), Paper CM3E.5*. (n.d.).
3. P. C. Konda, J. M. Taylor, and A. R. Harvey, "Scheimpflug multi-aperture Fourier ptychography : coherent computational microscope with gigapixels / s data acquisition rates using 3D printed components," in *Proc. SPIE 10076, High-Speed Biomedical Imaging and Spectroscopy: Toward Big Data Instrumentation and Management II, 100760R (February 22, 2017)* (n.d.).
4. L. Tian, Z. Liu, L.-H. Yeh, M. Chen, J. Zhong, and L. Waller, "Computational illumination for high-speed in vitro Fourier ptychographic microscopy," *Optica* **2**, 904 (2015).
5. P. C. Konda, J. M. Taylor, and A. R. Harvey, "Calibration and aberration correction in Multi-Aperture Fourier Ptychography," in *Imaging and Applied Optics 2016, OSA Technical Digest (Online) (Optical Society of America, 2016), Paper CT2D.2*. (n.d.).
6. L.-H. Yeh, L. Tian, Z. Liu, M. Chen, J. Zhong, and L. Waller, "Experimental robustness of Fourier Ptychographic phase retrieval algorithms," *Opt. Express* **23**, (2015).
7. P. C. Konda, J. M. Taylor, and A. R. Harvey, "High-resolution microscopy with low-resolution objectives: correcting phase aberrations in Fourier ptychography," in *Proc. SPIE 9630, Optical Systems Design 2015: Computational Optics, 96300X (September 23, 2015); doi:10.1117/12.2191338*. (n.d.).